

# Charge multiplication effect in thin diamond films

N. Skukan<sup>1,a)</sup>, V. Grilj<sup>1</sup>, I. Sudić<sup>1</sup>, M. Pomorski<sup>2</sup>, W. Kada<sup>3</sup>, T. Makino<sup>4</sup>, Y. Kambayashi<sup>3</sup>, Y. Andoh<sup>3</sup>, S. Onoda<sup>4</sup>, S. Sato<sup>4</sup>, T. Ohshima<sup>4</sup>, T. Kamiya<sup>4</sup>, M. Jakšić<sup>1</sup>

<sup>1</sup>*Division of Experimental Physics, Ruđer Bošković Institute, 10000 Zagreb, Croatia*

<sup>2</sup>*CEA-LIST, Diamond Sensors Laboratory, Gif-sur-Yvette F-91191, France*

<sup>3</sup>*Division of Electronics and Informatics, Faculty of Science and Technology, Gunma University, Kiryu, Gunma 376-8515, Japan*

<sup>4</sup>*National Institutes for Quantum and Radiological Science and Technology, Takasaki, Gunma 370-1292, Japan*

## Abstract

We report herein the enhanced sensitivity for the detection of charged particles in single crystal chemical vapour deposition (scCVD) diamond radiation detectors. The experimental results demonstrate charge multiplication in thin planar diamond membrane detectors, upon impact of 18 MeV O ions, under high electric field conditions. Avalanche multiplication is widely exploited in devices such as avalanche photo diodes, but has never before been reproducibly observed in intrinsic CVD diamond. Because enhanced sensitivity for charged particle detection is obtained for short charge drift lengths without dark counts, this effect could be further exploited in the development of sensors based on avalanche multiplication and radiation detector with extreme radiation hardness

Keywords: diamond, charge multiplication, avalanche, impact ionization

---

<sup>a)</sup> **Author to whom correspondence should be addressed. Electronic mail:** [nskukan@irb.hr](mailto:nskukan@irb.hr).

Because of its extraordinary physical characteristics, synthetic single crystal diamond is a promising material for future applications in various fields such as mechanics, optics and thermal management as well as power electronics and radiation detection. Particularly, radiation detectors based on scCVD diamonds can be found as beam profile monitors for both X-rays and high energy ions, dosimeters for radiotherapy and possible replacements for future upgrades of Atlas and CMS detectors because of their superior radiation hardness [1]. Electrical fields applied to scCVD diamond detectors are typically within a range from 0.1 to approximately 10 V/ $\mu\text{m}$  and most of the literature on charge carrier transport exploit even lower ranges of electric fields rarely reaching 2 V/ $\mu\text{m}$  [2, 3]. Values above these are seldom used because of the evolution of erratic leakage currents, causing an increase in noise and eventually an uncontrolled breakdown of the device. Although the theoretical dielectric strength of diamond material is extremely high, real samples suffer from dielectric breakdown at much lower electric field values [4].

A possible explanation for the discrepancies between the expected theoretical values and the experimentally used electric fields may lie in the structural defects within the diamond crystal lattice, potentially leading to a significant decrease of the high initial theoretical breakdown voltage [5]. Another practical explanation is that even for a relatively thin 100  $\mu\text{m}$  thick detector, an electric field of 100 V/ $\mu\text{m}$  requires a 10 kV bias voltage. Higher voltages are often not feasible and lead to discharges through vacuum feedthroughs, cables and surface currents on the device. However, possible avalanche multiplication which may be achievable at even higher electric fields, remains a physical effect of great interest to the electronic industry focused on diamond material. Proper knowledge of multiplication parameters will aid in the design of high voltage devices to optimize their geometry, doping and operating parameters. Furthermore, diamond detectors based on the avalanche principle are insensitive or less sensitive to visible light, which may be of great interest for sensor development and scientific community. Therefore, proper knowledge of the parameters ruling the avalanche process is desirable.

Charge multiplication in diamond has been tested by multiple groups on a variety of devices [6-9] with diverse results. However, none of these measurements were performed in intrinsic CVD diamond and only one addressed pulse mode multiplication, although the integration time used by the readout electronics did not exclude the photoconductive gain mechanism.

To avoid, or at least minimize the possibility of uncontrolled dielectric breakdown while measuring impact ionization multiplication in diamond, the device must be as thin as practically possible, preferably a film. To minimize the total number of defects, the active volume should also be minimized, i.e., the area under the electrodes must be small.

Following the development of a thin diamond membrane detector [10, 11], we tested its voltage holding capability and achieved 40 V/ $\mu\text{m}$  before erratic leakage current developed. The tested device was a 3.2  $\mu\text{m}$  thick membrane with 2x2 mm<sup>2</sup> area contacts. Although this electric field is already the highest applied for diamond radiation detectors, according to the theoretical calculations [12], at least 100 V/ $\mu\text{m}$  is needed to reach an amplification of only 5% and detector

thickness of several  $\mu\text{m}$ . Therefore, we decided to design a device of the same thickness, but with very minimal contact overlap.

The device under investigation was fabricated from standard grade ( $<1$  ppm N concentration), single crystal,  $<1\ 0\ 0>$  oriented CVD diamond produced by Element Six [13]. The sample was mechanically polished down to a  $30\ \mu\text{m}$  plate by Almax EasyLab [14]. Further thinning of the central portion of the sample to  $3\ \mu\text{m}$  was performed using an Ar/O plasma etching technique described in detail elsewhere [10]. A  $300\ \mu\text{m}$  wide Al strip electrode was sputtered on each side of the diamond membrane in a cross-like parallel plate geometry, resulting in a small overlap area of  $300 \times 300\ \mu\text{m}^2$  (Figure 1). The placement of the electrodes was carefully chosen under a high magnification optical microscope with birefringence imaging in a membrane region showing no evidence of bulk structural defects (birefringence contrast) or surface defects (pits) arising from polishing. Additionally, having such a small active area is beneficial for reducing the capacitance of the device, resulting in a higher bandwidth for fast transient current measurements. The sample was glued onto a specially designed printed circuit board with a via-hole in the central area to contain the transmission detector. An SMA connector was soldered to the board near the membrane. The top strip electrode was connected to the central pin of the SMA connector by  $60\ \mu\text{m}$  thick golden wire and silver-loaded conductive paste. The back strip electrode was grounded. In such a configuration the capacitance of the detector was estimated to be less than  $0.5\ \text{pF}$ . The thickness of the detector was estimated from the energy loss measurements using a telescope configuration with a silicon surface barrier E detector behind the diamond transmission detector, DeltaE. The final thickness of scCVD diamond membrane was measured to be  $3.25 \pm 0.1\ \mu\text{m}$  in the area of interest.

Prior to irradiation, dark I-V characteristics of the diamond detector were measured to assure the dielectric strength and absence of hard break-down. The device showed no leakage current ( $I < 100\ \text{fA}$ ) up to  $\pm 500\ \text{V}$  ( $154\ \text{V}/\mu\text{m}$ ). The device was not tested to the maximum voltage applied in later measurements to avoid hard breakdown before obtaining the data

The sample was mounted in the Rudjer Boskovic Institute ion microprobe [15] and irradiated by  $18\ \text{MeV}$  O ions in a low current mode (up to 1000 counts per second (cps) at maximum). The particular beam characteristics were chosen to fulfill the following requirements:

- The ions must traverse the entire sample to avoid polarization effect problems [16]
- Homogenous energy loss of ions throughout the depth of the sample, i.e., constant electron-hole pair creation
- The total amount of deposited energy must be high enough to enable the use transient current technique (TCT) [3] without the need for signal amplification and thus bandwidth limitation.

According to SRIM [17] simulation the total energy deposition in a  $3.25\ \mu\text{m}$  membrane of traversing  $18\ \text{MeV}$  O is approximately  $10.78\ \text{MeV}$  with a homogenous profile, which corresponds

to a total amount of 830,000 electron-hole pairs (~133 fC) per ion. As a result of nearly homogenous e-h pair creation along the ion track, the contribution of electrons and holes to the induced signal is equal; therefore, it is not possible to distinguish the difference between their multiplication phenomena. The charge collection efficiency (CCE) of the detector was mapped by the Ion Beam Induced Charge (IBIC) technique [18]. The beam current was maintained at a very low level of 100-1000 cps. The signal was collected and amplified with a charge sensitive preamplifier (Ortec 142A), followed by a shaping amplifier (Ortec 570). Data acquisition was performed by Canberra 8075 ADC units and homemade software [19]. The scans at lower voltages were approximately 500x500  $\mu\text{m}^2$  in size to observe the response of the entire active detector area, including the electrode edges. At high electric fields, the scanning area was decreased to approximately 150x100  $\mu\text{m}^2$  (placed in the central part of the electrodes) to avoid hard breakdown at the electrode edges where the strength of the electric field can be enhanced, which is initiated by ion impact. The total bias spanned from -640 to +650 V, which corresponds to an electric field of ~200 V/ $\mu\text{m}$ . This span of the electric field was greater than I-V measurements and eventually resulted in hard breakdown and microscopic bulk damage by the discharge at a bias of -650 V. The energy calibration of the measurement chain was performed with a silicon surface barrier detector and pulse generator. The CCE was calculated assuming an e-h pair creation energy of 13 eV [20] for diamond and 3.62 eV for silicon [21]. For the spectra recorded at different biases histograms were fitted with a Gaussian function and normalized to a calculated CCE. Figure 2. shows an overlap of the spectra at 100 V (~30 V/ $\mu\text{m}$ , 100% CCE) and 600 V (185 V/ $\mu\text{m}$ , proportional multiplication region). The position of the peak to the right corresponds to 2.2 times more collected charge, indicating the charge multiplication effect. The sigma of the peak is about 3 times larger, which is an indicator of higher statistical fluctuation because of the avalanching process [22]. Figure 3. shows the dependence of the (CCE) versus the electric field strength (E) . The plot essentially consists of three parts. At low electric fields, 0-3 V/ $\mu\text{m}$  in our case, the CCE is less than 100% and follows the Hecht equation [23]. A CCE of 3-30 V/ $\mu\text{m}$  asymptotically reaches 100% as expected and forms a plateau of almost constant efficiency. At higher electric fields, >30 V/ $\mu\text{m}$ , the CCE vs E dependence is exponential and exhibits a multiplication effect. According to McKay [24] and Chynoweth [25], the charge multiplication is parameterized by the multiplication factor  $\alpha$ , the number of new e-h pairs produced per one charge per one micron. Because we cannot distinguish between holes and electrons, the  $\alpha$  parameter is an average production value for both carriers. Following the derivation of McKay, a point charge,  $Q_0$ , generated at one electrode results, after passing the thickness,  $d$ , of the detector, in a total charge  $Q$  equal to:

$$Q = \frac{Q_0}{1 - \int_0^d \alpha x dx} \quad (1)$$

In our experiment the beam traversed through the entire detector. The induced e-h pairs were uniformly distributed over the thickness of the detector, forming charge density per unit length instead of a point charge. However, the electric field was constant. Every e-h pair, generated

primarily at position  $x$ , creates  $\alpha d$  new pairs before reaching end electrodes at 0 and  $d$ . These newly created pairs again have a chance  $\alpha d$  to create new pairs. Therefore, after an infinite number of such calculations the following equation is obtained:

$$Q = Q_0 + \alpha d Q_0 + (\alpha d)^2 Q_0 + \dots = Q_0 \sum_{i=0}^{\infty} (\alpha d)^i = \frac{Q_0}{1 - \alpha d} \quad (2)$$

Here, no recombination is taken into account and 100% CCE is assumed on the plateau. The relationship between the  $\alpha$  parameter and the electric field,  $E$ , can be empirically expressed in two ways. The first is to use the Chynoweth equation [25]:

$$\alpha = a e^{-\frac{b}{E}} \quad (3)$$

where  $a$  and  $b$  are fitting parameters. The second is to use the extended Chynoweth equation [4]:

$$\alpha = a e^{-\frac{b}{(E)^c}} \quad (4)$$

where the case of  $c=1$  corresponds to (3). In some other semiconductors, the  $c$  parameter has been shown to be different than 1 [26]. There is no physical significance in the parameters  $a$ ,  $b$  and  $c$ . Because the value of the  $c$  parameter in diamond is not established we fit the measured CCE to both (3) and (4). The fitting results are shown in Figures 3 and 4 and the parameters are listed in Table 1. Figure 3 shows that  $c=0.2$  fit better represents high electric field, but it fails at low electric fields (visible also in Figure 4). Different slopes of the fits show a large freedom for the expected value of  $\alpha$  at high electric fields. Figure 4 is the sum of all the theoretical and experimental work done in this area up to now. The measured multiplication parameter,  $\alpha$ , for the highest measured electric field of 200 V/ $\mu\text{m}$  in our experiment, equals approximately 1910  $\text{cm}^{-1}$  and fits well between the two theoretical curves from [4, 12, 27]. However, extrapolation to the higher electric fields gives lower expectation than any other work for  $\alpha$  parameter in that range.

$a [\mu\text{m}^{-1}]$	$b [\text{V}/\mu\text{m}]$	$c$
$0.56 \pm 0.03$	$216 \pm 9$	1
$180 \pm 31$	$19.7 \pm 0.5$	0.2

Table 1.

Fitting parameters for multiplication factor with two different equations

Equation (2) becomes divergent if  $\alpha \times d = 1$ . From this constraint, by extrapolation of the measured  $\alpha$  parameter, one may assume the avalanche breakdown (Geiger mode avalanche threshold) field, where quenching is needed to stop the avalanching process. For the usual two-parameter fit, as shown in equation (3), the calculation gives a threshold field of 363 V/ $\mu\text{m}$ , whereas the three-parameter fit (equation 4) gives a value of 285 V/ $\mu\text{m}$ , for this 3.25  $\mu\text{m}$  thick detector.

After reaching a hard breakdown for the charge sensitive measurements, the sample was remetallized using a similar procedure as described above, again selecting a defect-free region. Due to a number of defects and damage from previous breakdowns, the metallized area chosen was near the edge of the etched part of the sample. The measured energy loss of the traversing ions through the sample in this area was  $15.1 \pm 1$  MeV which corresponds to about  $4.25 \pm 0.3$   $\mu\text{m}$ . To confirm the sub-nanosecond avalanche process and exclude the photoconductive gain effect, we performed a Transient Current Technique [3] measurement using only a bias TEE and Lecroy WaveMaster 8500; 5 GHz, 20 Gs/s digital storage oscilloscope. To protect the oscilloscope from damage, we limited the bias span for the transient current measurements to 300 V, the value at which hard breakdown is less probable and the multiplication process is evident from charge sensitive measurements. The measured transient current signals are presented in Figure 5, where each trace is an average of a few hundred single shots measured at 40V, 80V and 300V bias voltages. Even at the lowest, 40 V bias ( $\sim 9.4$  V/ $\mu\text{m}$ ), the charge carrier velocities are almost saturated. Therefore, any increase in current amplitude with bias increase is an indication of an avalanche multiplication. However, because of the poor 50 ohm impedance matching, strong ringing of the signals was observed. Taking into account the saturation velocity of both charge carriers ( $1.2 - 2.7 \times 10^7$  cm/s) [28] the intrinsic charge transit time was less than 40 ps for a 4.25  $\mu\text{m}$  drift path. Such short signals are quite challenging in terms of readout electronics and electrical connection bandwidth. Approximately 18 GHz bandwidth would be needed to observe directly intrinsic transient current signals, which was beyond the limits of the current experimental set-up. The 10-90% rise time of all the signals was approximately 170 ps, corresponding to a 2 GHz bandwidth which is less than the 5 GHz bandwidth of the digital storage oscilloscope. The observed bandwidth limitation is most likely related to the inductance of the bonding wire connecting the upper contact and can be improved in future experiments. Nevertheless, identical rise and fall times of all three signals and progressively increasing amplitude, indicate a fast avalanching process related to the impact ionization rather than photoconductive gain. The latter is the injection of charge carriers through the ohmic contact in order to compensate the opposite charge that remained inside the device (due to trapping and slower collection of one carrier) after the faster carrier is collected. The photoconductive gain is proportional to the lifetime and inversely proportional to the transit time of the charge carriers in the device, therefore it has a relatively long time constant, approaching the life time of charge carriers in the tested material (a few ns in our case). More details about the photoconductive gain mechanism can be found in [21] and photoconductive gain in diamond detectors in [29]. The observed effect can find a practical application at the current stage in detection techniques, i.e., time measurements with higher signal to noise ratio.

209

210 In conclusion, we have directly observed avalanche multiplication in a thin diamond detector.  
211 Ionization coefficients were fitted to the experimental data and the minimum electric field for the  
212 Geiger mode avalanche was determined. Compared to non-amplified signals, the TCT  
213 measurements showed no long component of the multiplied signal related to photoconductive  
214 gain, which supports the theory of an impact avalanche. The approach presented in this work  
215 opens the possibility for the development of devices based on the avalanche principle as well as a  
216 method to measure avalanche ionization coefficients for a better theoretical description of the  
217 charge carrier transport in diamond material. Similar effect of charge multiplication is observed  
218 on other diamond membranes, by irradiation with a number of different ion species. A more  
219 detailed paper covering these is under preparation.

220

## 221 References

222 [1] A. Oh, J. Inst. 10, C04038 (2015)

223 [2] M. Pomorski, E. Berdermann, W. de Boer, A. Furgeri, C. Sander, and J. Morse, Diamond  
224 Relat. Mater. 16, 1066 (2007)

225 [3] H. Pernegger, S. Roe, P. Weilhammer, V. Eremin, H. Frais-Kolbl, K. E. Griesmayer, H.  
226 Kagan, S. Schnetzer, R. Stone, W. Trischuk, D. Twitchen, and A. Whitehead, J. Appl. Phys. 97,  
227 073704 (2005)

228 [4] A. Hiraiwa, and H. Kawarada, J. Appl. Phys. 114, 034506 (2013)

229 [5] M. Suzuki, T. Sakai, T. Makino, H. Kato, D. Takeuchi, M. Ogura, H. Okushi and S.  
230 Yamasaki, Phys. Status Solidi A 210, 2035 (2013)

231 [6] V. Mortet and A. Soltani Appl. Phys. Lett. 99, 202105 (2011)

232 [7] J. Isberg, M. Gabrysch, A. Tajani, and D. J. Twitchen, Adv. Sci. Technol. 48, 73 (2006)

233 [8] E. A. Konorova, Yu. A. Kuznetsov, V. F. Sergienko, S. D. Tkachenko, A. V. Tsikunov,

234 A. V. Spitsyn, Yu. Z. Danyushevskii, Sov. Phys. Semicond. 17, 146 (1983).

235 [9] M. Irie, S. Endo, C. L. Wang, T. Ito, Diam. Rel. Mat. 12, 1563 (2003).

236 [10] M. Pomorski, B. Caylar, and P. Bergonzo, Appl. Phys. Lett. 103, 112106 (2013).

237 [11] V. Grilj, N. Skukan, M. Pomorski, W. Kada, N. Iwamoto, M. Jakšić, T. Kamiya, Appl. Phys.

238 Lett. 103, 243106 (2013).

239 [12] T. Watanabe, M. Irie, T. Teraji, T. Ito, Y. Kamakura, and K. Taniguchi, Jpn. J. Appl. Phys.,

240 Part 2 40, L715 (2001).

241 [13] Element Six Ltd, King's Ride Park, Ascot, Berkshire SL5 8BP, UK

242 [14] <http://www.almax-easylab.com/>

243 [15] M. Jakšić, I. Bogdanović-Radović, M. Bogovac, V. Desnica, S. Fazinić, M. Karlusić, Z.

244 Medunić, H. Muto, Z. Pastuović, Z. Siketić, N. Skukan and T. Tadić, Nucl. Instrum. Methods

245 Phys. Res. B 260, 114 (2007).

246 [16] V. Grilj, N. Skukan, M. Jakšić, M. Pomorski, W. Kada, T. Kamiya, T. Ohshima, Nucl.

247 Instrum. Methods Phys. Res. B **372**, 161 (2016)

248 [17] [www.srim.org](http://www.srim.org)

249 [18] M.B.H. Breese , E. Vittone , G. Vizkelethy, P.J. Sellin, Nucl. Instrum. Methods Phys. Res.

250 B 264, 345 (2007)

251 [19] M. Bogovac, I. Bogdanović, S. Fazinić, M. Jakšić, L. Kukec and W. Wilhelm, Nucl.

252 Instrum. Methods Phys. Res. B **89**, 219 (1994)



253 [20] L. S. Pan, S. Han, and D. R. Kania, Diamond: Electronic Properties and Applications.  
 254 Kluwer Academic, Dordrecht, 1995.

255 [21] G. F. Knoll, Radiation Detection and Measurements, Third Edition, John Wiley &  
 256 Sons, 2000

257 [22] R. J. McIntyre IEEE Trans. Electron Devices. 30, 164 (1966)

258 [23] K. Hecht, Zeitschrift für Physik, 77, 235 (1932) [24] K. G. McKay, Phys. Rev. 94, 877 (1954)

259 [25] A. G. Chynoweth Phys. Rev. 109 1537 (1958)

260 [26] F. Bertazzi, M. Moresco, and E. Bellotti, J. Appl. Phys. 106, 063718 (2009).

261 [27] A. Hiraiwa and H. Kawai J. Appl. Phys. 117, 124503 (2015)

262 [28] M. Pomorski, Doctoral Dissertation, Frankfurt 2008

263 [29] P. Bergonzo, R.B. Jackman (Chapter 6 authors), C. Nebel, J. Ristein (editors): Thin-Film  
 264 Diamond II Academic Press, 2004,

265

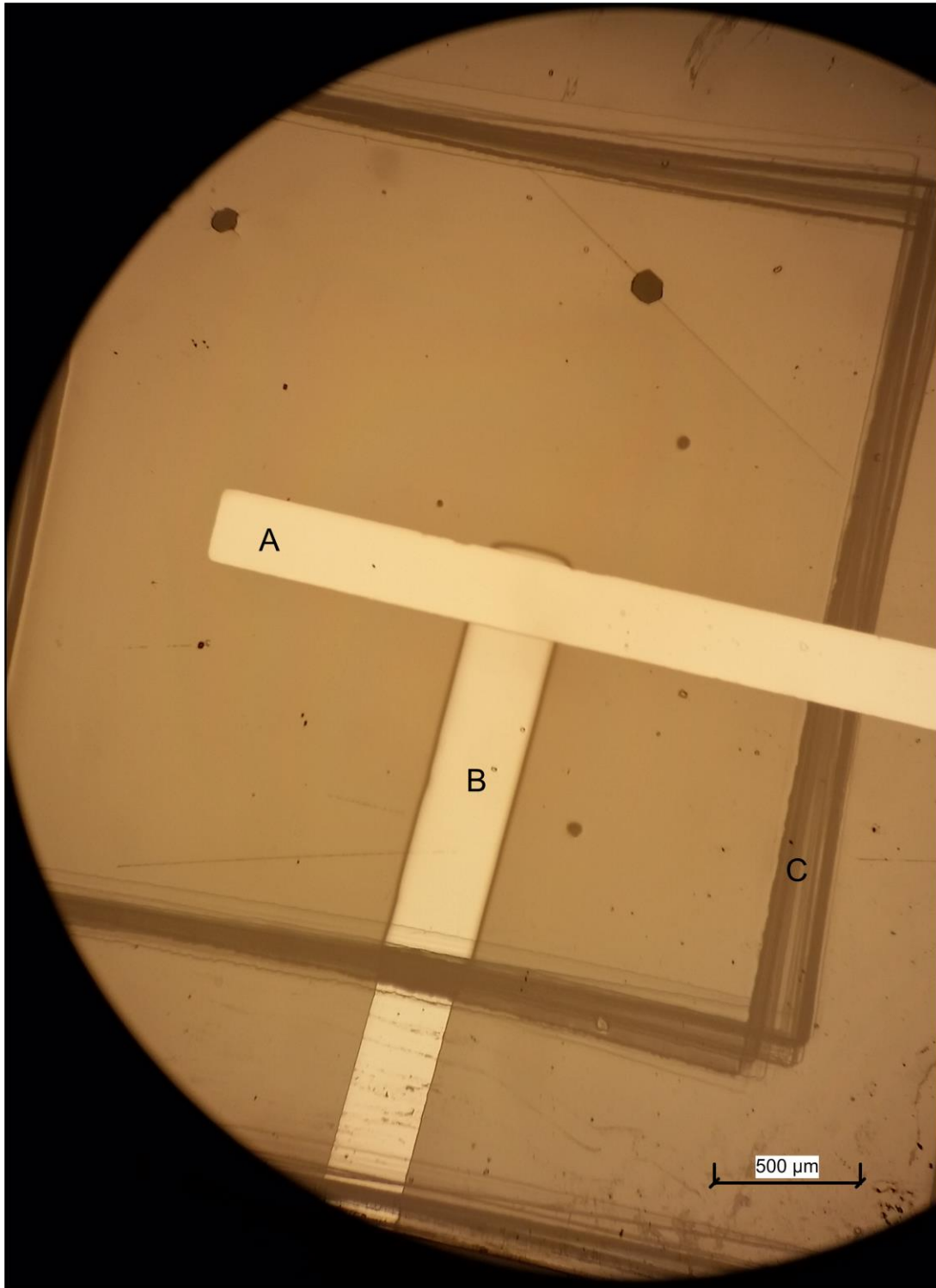


Figure 1. Microscope image of 3.25  $\mu\text{m}$  thick scCVD diamond-membrane detector electrode configuration. (A): upper electrode, (B): lower electrode, (C): the edge of the etched area

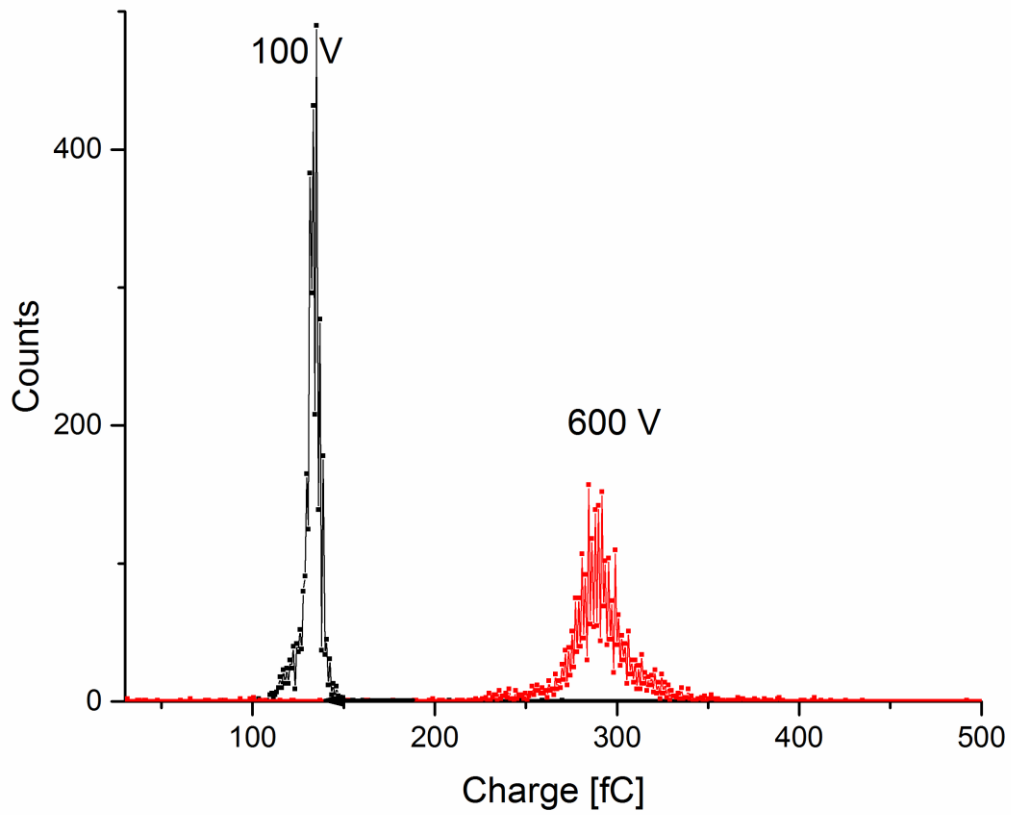


Figure 2. Measured energy loss spectra of 18 MeV O ion traversing the diamond-membrane. 100V bias voltage (30 V/ $\mu\text{m}$ ) and 600 V bias voltage (184 V/ $\mu\text{m}$ ). A  $\times 2.2$  collected charge multiplication is evidenced for the 600 V bias. The integral of both peaks is  $\sim 3500$  counts.

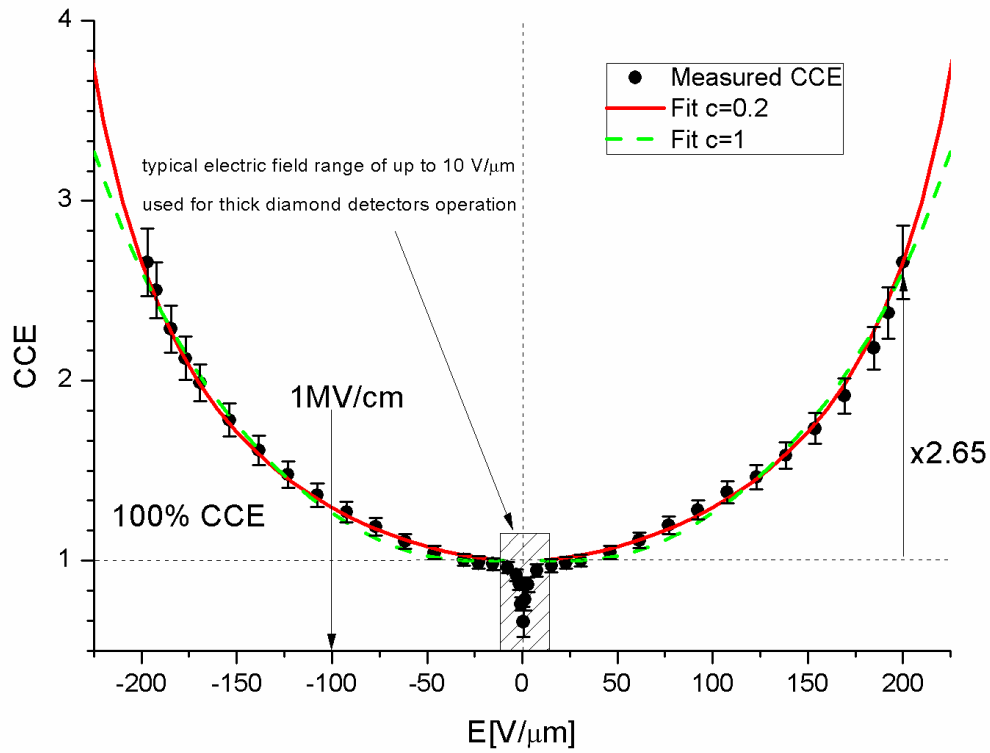


Figure 3. Electric field vs charge collection efficiency, where the black dots are measured points, the green line is a fit with the parameter  $c=1$  and the red line represents fit with  $c=0.2$ . The patterned rectangular represent the typical range of operation for thick diamond detectors

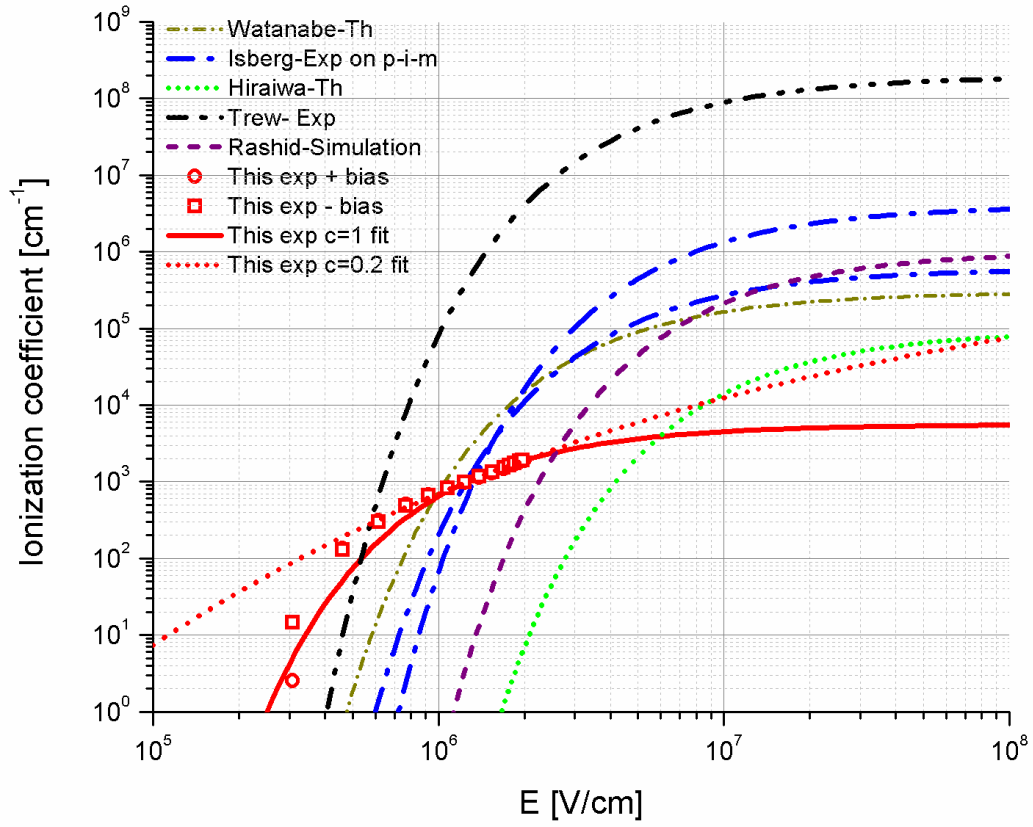


Figure 4. Comparison of  $\alpha$  ionization parameter for different references and the present experiment. The solid red line represents the standard fit with  $c=1$ . The dashed red line is the fit with  $c=0.2$ . The data for the comparison were taken from [27] and references inside.

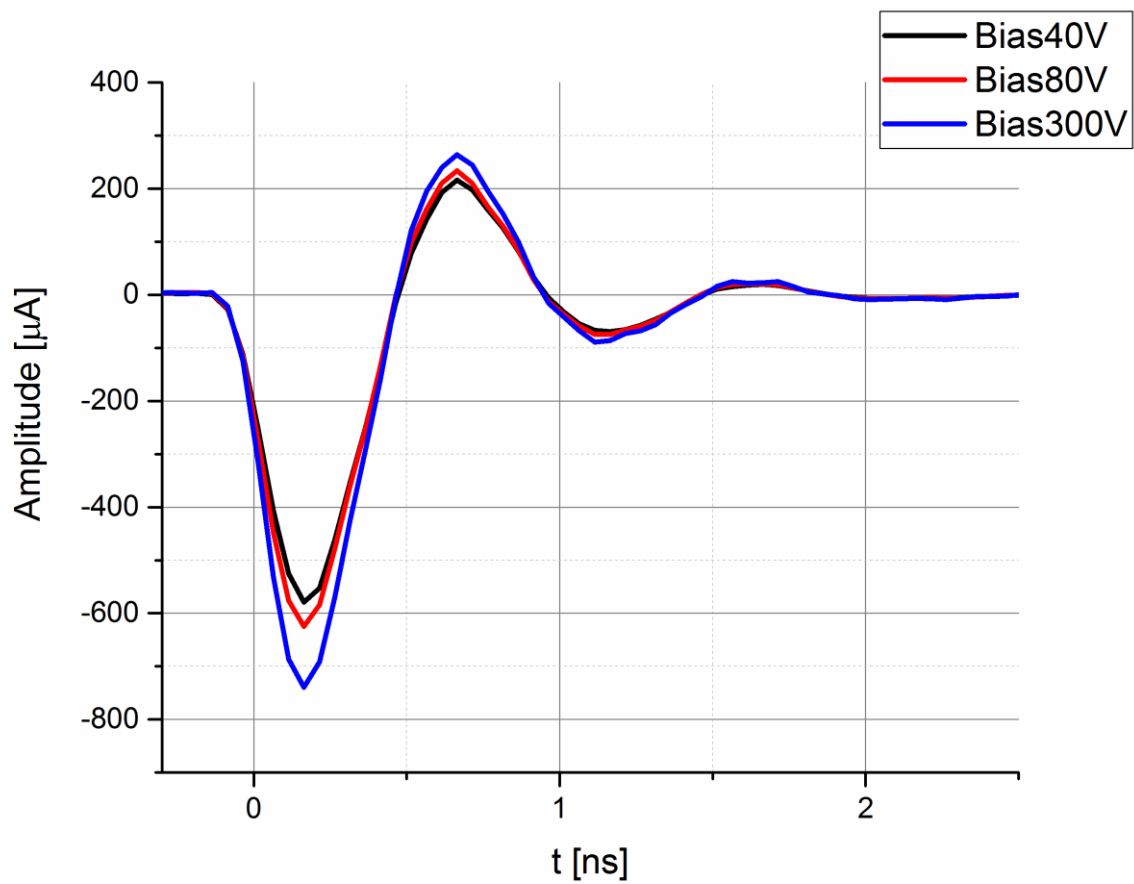


Figure. 5. Average over a few hundred single shots transient current signals for three different biases: 40V (9.4 V/ $\mu\text{m}$ -beginning of the 100% CCE plateau), 80 V (18.8 9.4 V/ $\mu\text{m}$ -plateau) and 300 V (70.5 9.4 V/ $\mu\text{m}$ -multiplication regime). The curves are moved in time to better express equal shape of the traces.